

Dear Author,

Please, note that changes made to the HTML content will be added to the article before publication, but are not reflected in this PDF.

Note also that this file should not be used for submitting corrections.



Contents lists available at ScienceDirect

## Agriculture, Ecosystems and Environment

journal homepage: [www.elsevier.com/locate/agee](http://www.elsevier.com/locate/agee)1 Historical tracking of nitrate in contrasting vineyards using water  
2 isotopes and nitrate depth profiles3 **Q1** Matthias Sprenger<sup>a,\*</sup>, Martin Erhardt<sup>b</sup>, Monika Riedel<sup>b</sup>, Markus Weiler<sup>a</sup>4 <sup>a</sup>Chair of Hydrology, Faculty of Environment and Natural Resources, Albert Ludwig University of Freiburg, Fahnbergplatz, 79098 Freiburg, Germany5 <sup>b</sup>State Institute for Viticulture and Enology, Merzhauser Str. 119, 79100 Freiburg, Germany

## ARTICLE INFO

## Article history:

Received 12 August 2015  
Received in revised form 10 February 2016  
Accepted 12 February 2016  
Available online xxx

## Keywords:

Soil hydrology  
Isotope hydrology  
Nitrate leaching  
Groundwater protection  
Viticulture

## ABSTRACT

The European Water Framework Directive (EWFd) aims to achieve a good chemical status for the groundwater bodies in Europe by the year 2015. Despite the effort to reduce the nitrate pollution from agriculture within the last two decades, there are still many groundwater aquifers that exceed nitrate concentrations above the EWFd threshold of 50 mg L<sup>-1</sup>. Viticulture is seen as a major contributor of nitrate leaching and sowing of a green cover was shown to have a positive effect on lowering the nitrate loads in the upper 90 cm of the soil. However, the consequences for nitrate leaching into the subsoil were not yet tested. We analyzed the nitrate concentrations and pore water stable isotope composition ( $\delta^2\text{H}$ ) to a depth of 380 cm in soil profiles under an old vineyard and a young vineyard with either soil tillage or permanent green cover in between the grapevines. The pore water  $\delta^2\text{H}$  data was used to calibrate a soil physical model, which was then used to infer the age of the soil water at different depths. This way, we could relate elevated nitrate concentrations below an old vineyard to tillage processes that took place during the winter two years before the sampling. We further showed that the elevated nitrate concentration in the subsoil of a young vineyard can be related to the soil tillage prior to the planting of the new vineyard. If the soil was kept bare due to tillage, a nitrate concentration of 200 kg NO<sub>3</sub><sup>-</sup>-N ha<sup>-1</sup> was found in 290–380 cm depth 2.5 years after the set-up of the vineyard. The amount of nitrate leaching was considerably reduced due to a seeded green cover between the grapevines that took up a high share of the mineralized nitrate reducing a potential contamination of the groundwater.

© 2016 Published by Elsevier B.V.

6 **1. Introduction**

7 At least since the EU council adopted the Nitrates Directive over  
8 two decades ago the members of the European Union commit  
9 themselves to reduce the nitrate pollution of European water  
10 bodies by agricultural sources (European Council, 1991). This goal  
11 was affirmed by the EU Water Framework Directive, whose  
12 integrated river basin management aimed to get the groundwater  
13 in Europe into a “good chemical status” by 2015 (European Council,  
14 2000). The upper limit of 50 mg L<sup>-1</sup> for nitrate in groundwater was  
15 confirmed by the Groundwater Directive (European Council,  
16 2006). However, despite the efforts in the last two decades, many  
17 groundwater aquifers do not meet the quality standard of the EU  
18 due to elevated nitrate concentrations. In agriculturally intense  
19 catchments in the southwest of Germany, several groundwater  
20 monitoring wells show nitrate concentrations that exceed the

threshold of 50 mg L<sup>-1</sup> and at some sampling locations, there is  
even an increasing trend (LUBW, 2009). The situation of the  
groundwater quality only improves slowly around the Kaiserstuhl  
located west of Freiburg i. Br., Germany, even though the average  
nitrate surplus decreased between 1980 and 2005 from 24 to  
11 kg N ha<sup>-1</sup> and the average nitrate loads of leaching water  
declined from 57.9 mg L<sup>-1</sup> in 1980 to 29.8 mg L<sup>-1</sup> in 2005 (LUBW,  
2008). Nevertheless, vine farming is seen as a relevant factor  
influencing high nitrate concentrations (Erhardt and Riedel, 2011).  
Under old vineyards in the study area, the nitrate-N concentrations  
in the upper 90 cm of soil are on average far below the control value  
of 90 kg N ha<sup>-1</sup> defined by the Umweltministerium (2001). The  
concentration in the topsoil shows a decreasing trend for the  
monitoring period between 2001 and 2013 (LTZ, 2013). However,  
under young vineyards the nitrate-N concentrations are on average  
above the threshold in the first year (Erhardt et al., 2012). The  
elevated nitrate-N concentrations result from high Nitrate  
mineralization rates of organic matter developed in the previous  
vineyard and deeper soil tillage (e.g., land clearing and soil  
modification) as well as shallow soil tillage before and after  
planting (Erhardt et al., 2012; Rupp, 1988). These values decrease

**Q3**

\* Corresponding author.

E-mail addresses: [matthias.sprenger@abdn.ac.uk](mailto:matthias.sprenger@abdn.ac.uk), [Matthias-Sprenger@gmx.de](mailto:Matthias-Sprenger@gmx.de)  
(M. Sprenger).

<http://dx.doi.org/10.1016/j.agee.2016.02.014>

0167-8809/© 2016 Published by Elsevier B.V.

over the following years and approach the nitrate concentrations of old vineyards after about four years (Erhardt and Riedel, 2013). Thus, a possible nitrate leaching from vineyards is most likely within the first year after planting the grapevines. The concentration of nitrate under young vineyards can considerably be reduced by sowing a mixture of *Phacelia tanacetifolia* and *Fagopyrum esculentum* and *Sinapis alba* in between the rows of grapevines instead of keeping a bare soil due to tillage (Erhardt and Riedel, 2013). The green cover, sown in every second interrow one month after planting, did not have any consequences regarding the growth of the young vine plants in the first year (Erhardt and Riedel, 2012; Erhardt et al., 2013).

These studies dealing with an optimal nitrate supply of the grapevines in the topsoil, while keeping the contamination of groundwater by nitrate leaching low are promising. However, it is yet unknown if the lowered nitrate concentration in the upper 90 cm due to sowing in the interrows on a vineyard also positively influences the leaching of nitrate into the deeper soil eventually reaching the groundwater. Soil physical modeling, including pore water stable isotope data ( $\delta^{2}\text{H}$ ) as a natural tracer for calibrating the soil water balance and travel times, was shown to enable tracing the water movement into deeper soil layers (Sprenger et al., 2015). Though, a practical application and a validation with another tracer have not been done so far. Based on the above mentioned experiences and knowledge gaps we test the following hypothesis in this study:

- i.) The timing of the nitrate mineralization can be traced back by pore water  $\delta^{2}\text{H}$  data.
- ii.) The risk of nitrate leaching into the subsoil is higher under young vineyards than under old vineyards
- iii.) A permanent green cover reduces the nitrate loads in the subsoil.
- iv.) Soil tillage in winter increases the risk of nitrate leaching.

Our objective is to investigate the nitrate-N concentrations in parallel with pore water  $\delta^{2}\text{H}$  data in the soil down to a depth of 380 cm. The pore water  $\delta^{2}\text{H}$  measurements will be used to infer the water age in the soil to potentially relate an elevated nitrate signal at a certain depth to the time the isotopic signal of the water was introduced by the rainwater.

## 2. Methods

### 2.1. Study site

The study was conducted in the catchment of the groundwater aquifer Freiburger Bucht in the west of Freiburg i. Br., Germany, where the groundwater body showed a nitrate concentration above the legal limit of  $50\text{ mg L}^{-1}$ . Vineyards are holding a relatively high share of 12% of the catchment area and are often established on terraces. The prevailing climate is temperate and for the years 2008–2013, the annual average air temperature was  $10.5^{\circ}\text{C}$  and the annual rainfall was 722 mm. With about 17 frost days per year, snow does only occur occasionally. The studied soils are silty Pararendzina on deep Pleistocene loess. The soil profile is divided into a humus plowing horizon (Ap) in the upper 30 cm and a relatively uniform parent material below. Investigations were conducted in an old and a young vineyard, which are located in about 3 km distance from each other. The old vineyard was established in 1998.  $70\text{ kg N ha}^{-1}$  of N-fertilization was applied by sulfate of ammonia in the years 2011–2013. Two different management practices were investigated: on the one hand, a permanent green cover in between the grapevines (OldGC), and on the other hand green cover with surface tillage and seeded green cover in every 2nd interrow, which shifted every other year

(OldST). The young vineyard was planted in May 2011. No fertilization was done in 2011, but sulfates of ammonia were applied to add  $30\text{ kg N ha}^{-1}$  in 2012 and  $50\text{ kg N ha}^{-1}$  in 2013. Similar to the old vineyards, the management practice at young vineyards was studied. At one site, a permanent green cover with a mixture of *P. tanacetifolia* and *F. esculentum* and *S. alba* was sown in every second interrow one month after planting the vineyards (NewGC). In every other row a green cover was seeded four months after the planting of the grapevines. In this study, the latter interrows were not considered. At the other study site in the young vineyard, the soil was kept bare with surface tillage in the first year (NewST). An overview of the management practice and schedule for the years 2010–2012 at the four different sites is given in Table 1.

### 2.2. Soil sampling

Soil sampling was conducted on the 4th and 5th of November 2013 at the young and old vineyards, respectively. At each of the four study sites, soil cores with a diameter of 8 cm to a depth of 380 cm were drilled. Soil sampling was done in approximately 5 cm intervals and of each sample of approximately  $265\text{ cm}^3$  volume about 40 g were taken for the nitrate analysis and the remaining ca. 250 g were used to determine the  $\delta^{2}\text{H}$  of the pore water. The soil samples for the nitrate analysis were cooled after the sampling and stored frozen at  $-20^{\circ}\text{C}$  until analysis. The nitrate analyses were done according to LTZ (2001) and values of  $\text{kg NO}_3^{-}\text{-N ha}^{-1}$  were obtained by assuming a bulk density of 1.3 in the upper 30 cm and 1.5 below 30 cm. Since a green cover was sown only in every second interrow, but only the interrow of the green cover was sampled in NewGC, an upscaling of the point sampling into space is not possible. The pore water  $\delta^{2}\text{H}$  analyses were done according to Wassenaar et al. (2008) as described in more detail by Sprenger et al. (2015). The measured isotopic signal is given as  $\delta^{2}\text{H}$  in [‰] relative to the Vienna Standard Mean Ocean Water (VSMOW). The

**Table 1**

Overview of the different management practices at the studied vineyards for the years 2010–2012.

Year	Date	Management practice	OldGC	OldST	NewGC	NewST	
2010	Oct.	Vineyard removal			X	X	
	8th Nov.	Plow (25 cm)			X	X	
2011	27th April	Disc harrow (3 cm)			X	X	
	29th April	Power harrow (7 cm)			X	X	
	3rd May	Planting of vineyards			X	X	
	3rd May	Mulching	X	X			
	4th May	Rotary hoe		X			
	21st May	Power harrow (7 cm)			X	X	
	31st May	Sowing		X	X		
	15th June	Mulching	X	X			
	20th June	Power harrow (7 cm)				X	
	4th July	Mulching	X	X			
2012	11th Aug.	Power harrow (7 cm)				X	
	2nd Sept.	Power harrow (7 cm)				X	
	24th Sept.	Mulching	X	X			
	29th Dec.	Disc harrow		X			
	2012	26th April	Mulching	X	X		
		30th April	Power harrow (2 cm)			X	X
		2nd May	Power harrow (6 cm)		X		
		3rd May	Sowing		X		
		23rd May	Mulching			X	
		6th June	Mulching	X	X		
15th June		Mulching			X		
20th June		Power harrow (6 cm)				X	
26th June		Power harrow (6 cm)				X	
17th July		Mulching	X	X			
18th July	Mulching			X	X		
5th Sept.	Mulching	X	X				

precision for the pore water  $\delta^2\text{H}$  analyses is 1.16‰ and defined here as the average standard deviation during two-minute long measurements of the headspace that was in isotopic equilibrium with the pore water. The vapor was directly sampled with a wavelength-scanned cavity ring down spectrometer (WS-CRDS, Picarro, Santa Clara, USA).

### 2.3. Pore water age dating

In order to infer the water age of the pore water sampled in the early November 2013, we used the soil physical model HYDRUS-1D (Šimůnek et al., 2012). The transient water flow was simulated by numerically solving the Richards equation. The required soil hydraulic parameters that describe the water retention and hydraulic conductivity function in according to the Mualem–van Genuchten model are (van Genuchten, 1980): the residual and saturated volumetric water contents ( $\theta_r$  [ $\text{L}^3 \text{L}^{-3}$ ] and  $\theta_s$  [ $\text{L}^3 \text{L}^{-3}$ ], respectively), the inverse of the capillary fringe thickness ( $\alpha$  [ $\text{L}^{-1}$ ]), two shape parameters ( $n$  [–], and  $m$  [–], where  $m = 1 - 1/n$ ), and the saturated hydraulic conductivity ( $K_s$  [ $\text{LT}^{-1}$ ]). We simulated the transport of  $\delta^2\text{H}$  according to the advection–dispersion model, which requires the dispersivity parameter  $\lambda$  [cm]. Since  $\delta^2\text{H}$  is usually negative in rainwater and pore water, an arbitrary offset (+100‰) was added to get positive values. The potential evapotranspiration was estimated by the Hargreaves Formula, partitioning of the evapotranspiration was done according to the estimated surface cover fraction of the vineyards (Beers law, Ritchie (1972)), and the root water uptake was simulated according to the Feddes model (Feddes et al., 1978), with parameters for grapevines given by Wesseling (1991). The surface cover fraction of the vegetation on the study sites was assumed to be 0.1 for the dormant season (1st November–1st of March) and 0.7 for the growing season (1st of May–1st of September). In the transition period, a linear increase and decrease, respectively, of the surface cover fraction was assumed. The maximum rooting depth was estimated from the soil cores to be 100 cm for the old vineyards. For the time period between November 2010 and May 2011, the rooting depth was set zero for NewST and NewGC, because of the demolition of an established vineyard and the set-up of a new vineyard at these sites. Rooting depth was assumed to increase to 60 cm by September 2011, to 80 cm by June 2012, and to be at 100 cm from August 2012 onwards. The root distribution was assumed to decrease exponentially in accordance to Hoffman and van Genuchten (1983). Snow fall was considered and the snow melt was modeled by a degree-day method. The upper boundary of the model was defined by the precipitation input and evapotranspiration output, while the  $\delta^2\text{H}$  data was represented by flux concentrations in the precipitation (Fig. 1) and evapotranspiration. Since solute flux concentrations in the evaporating water are usually not accounted for in the HYDRUS code, we used a modified code according to Stumpp et al. (2012) in this study. The lower boundary was defined as a free drainage including flux concentration of  $\delta^2\text{H}$ . As initial conditions, we chose a soil moisture of  $0.15 \text{ cm}^3 \text{ cm}^{-3}$  as sampled in the soil core for the subsoil and a  $\delta^2\text{H}$  of  $-57\text{‰}$ , which is the weighted average of the precipitation input. The isotopic composition of the precipitation was sampled in a vineyard in ca. 12 km distance in Eichstetten between June 2011 and July 2013. Isotope data from rainfall at the Schauinsland was taken for the period September 2008–June 2011. Since the Schauinsland is at about 1000 m higher altitude than the study sites, the isotope data was corrected for elevation effects by linear regression with data from Eichstetten ( $r^2 = 0.77$ ). The precipitation and the air temperature were measured at a meteorological station ca. 3 km away (Opfingen). For the simulation, the 380 cm soil profile was discretized into 101 nodes with higher node density at the top of the soil profile. Since the soil survey showed no

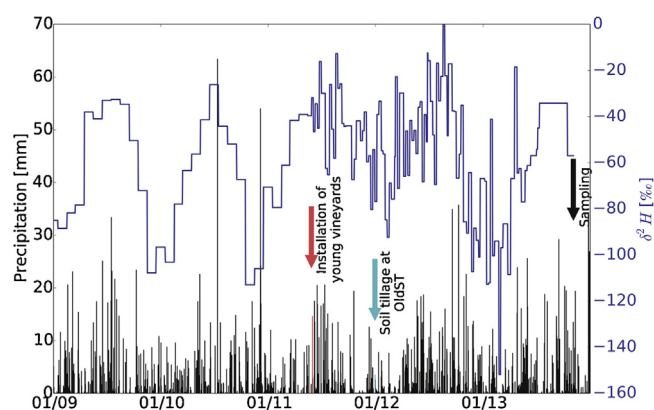


**Fig. 1.** Time series of daily rainfall and its monthly or bi-weekly deuterium composition  $\delta^2\text{H}$ . The arrows show the timing of the set-up of the young vineyards (red, 24th of May 2011), the timing of the soil tillage at one of the old vineyards (blue, 30th of December 2011), and the timing of the sampling of nitrate concentrations and water stable isotopes of the pore waters (4th and 5th of November 2013). (For interpretation of the references to color in this figure legend, the reader is referred to the web version of this article.)

pronounced differences of the texture over depth, no horizontalization was done for the model setup. Thus, the number of required soil hydraulic parameters was 6.

These six parameters were calibrated by fitting the simulated to the observed pore water  $\delta^2\text{H}$  profiles. The objective function describing the model efficiencies of each parameter set was defined according to the Kling–Gupta–efficiency (Kling et al., 2012). The best parameter set was searched within a defined parameter space by the Shuffled Complex Evolution algorithm (Duan et al., 1994). For more details regarding the model setup and calibration, the reader is referred to (Sprenger et al., 2015).

In order to determine the fate of the rain water in the simulation period between 2009 and 2013, we tracked the precipitation of each rainy day with a virtual tracer as proposed by Sprenger et al. (2015). The transport of the virtual ideal tracer was simulated in a forward mode with the site specific calibrated HYDRUS-1D model. In accordance to Sprenger et al. (2016), the median of the tracer breakthrough curves at 100 cm depth was calculated for every precipitation input, which defines the time variable median travel time of the recharge (mTT), as this depth is the maximum root zone in the model. The maximum of the cumulative tracer breakthrough curves gives for each rainy day the partitioning between recharge and evapotranspiration of the input water ( $Q/P$ ). For selected rainy days, we traced the fate of the rain water in the profile to show the distribution of the water over the soil depth at the beginning of November 2013, when the nitrate profiles were taken. In Fig. 1, we show exemplary the timing of the first rain event after the sowing of the green cover was done a month after the set-up of the young vineyards (31st of May 2011) and of the first rain after soil tillage at the old vineyards (30th of December 2011). The precipitation of these two dates was traced for the young vineyards (NewST and NewGC) and the old vineyard where soil tillage was done (OldST), respectively.

## 3. Results

### 3.1. Nitrate-N concentrations

The total nitrate concentrations of the upper 90 cm for all study sites was clearly below the threshold of  $90 \text{ kg NO}_3^- \text{-N ha}^{-1}$  as defined for the upper 90 cm by the Umweltministerium (2001). At all sites, except OldGC, the nitrate concentrations decreased within the first 50 cm to values below  $0.5 \text{ kg NO}_3^- \text{-N ha}^{-1}$  for the 5 cm

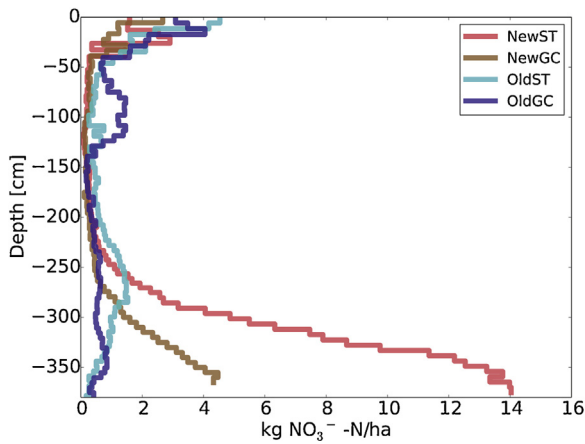


**Fig. 2.** Nitrate-N depth profiles on the 4th and 5th of November 2013 under vineyards in yield with permanent green cover in between the rows of grapevines (OldGC) or periodical soil tillage in the rows (OldST) and new established vineyards with permanent green cover in between the rows of grapevines (NewGC) or bare soil due to soil tillage in the rows (NewST). Sampling interval was approx. 5 cm.

intervals and stayed that low until 200 cm depth (Fig. 2). Between 200 and 350 cm, OldST showed elevated nitrate concentrations, peaking at 270 cm depth with  $1.8 \text{ kg NO}_3^- \text{-N ha}^{-1}$ . From 250 cm on, the nitrate concentrations of both NewST and NewGC rose over the depths and peaked at the lower end of the profiles. The increase in nitrate started higher in the profile and the increase was more pronounced for NewST than for NewGC. At NewST, the nitrate concentration reached a maximum of  $14 \text{ kg NO}_3^- \text{-N ha}^{-1}$  and the nitrate concentration peaked for NewGC at  $4.3 \text{ kg NO}_3^- \text{-N ha}^{-1}$ . For both sites under young grapevines, it was not clear if the nitrate concentration increased further below the maximum sampling depth of 380 cm. There were in each of the four sampled profiles

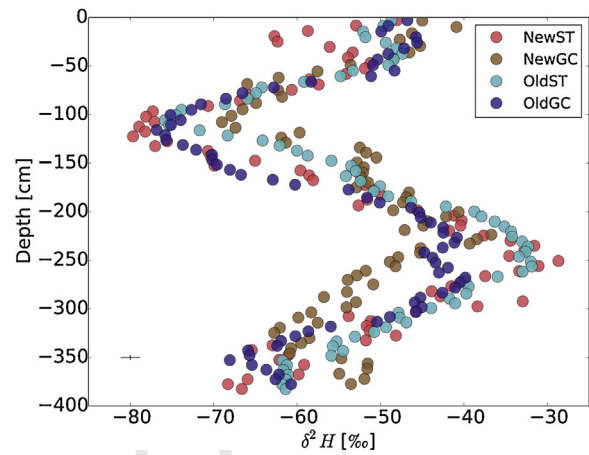


**Fig. 3.** Isotopic signal  $\delta^2\text{H}$  in pore waters for the four different studied soils on the 4th and 5th of November 2013. The accuracy of the  $\delta^2\text{H}$  analyses as the average standard deviation is shown with error bars below the legend.

peaks of nitrate concentrations that had elevated values compared to the same depths at the other sites.

### 3.2. Stable isotope composition

The pore water  $\delta^2\text{H}$  profiles showed all a sinusoidal variation (Fig. 3). One peak of depleted  $\delta^2\text{H}$  of  $-70$  to  $-80\text{‰}$  was present for all four sites between  $-100$  and  $-120$  cm. The peaks of enriched  $\delta^2\text{H}$  of  $-30$  to  $-43\text{‰}$  were less pointed, but wider than the first one and was between  $-220$  and  $-270$  cm. Another peak of depleted  $\delta^2\text{H}$  was between  $330$  and  $380$  cm depth, where the  $\delta^2\text{H}$  values were about  $10\text{‰}$  higher than for the upper peak ( $-60$  to  $-70\text{‰}$ ). NewGC showed generally a slightly more dampened signal than

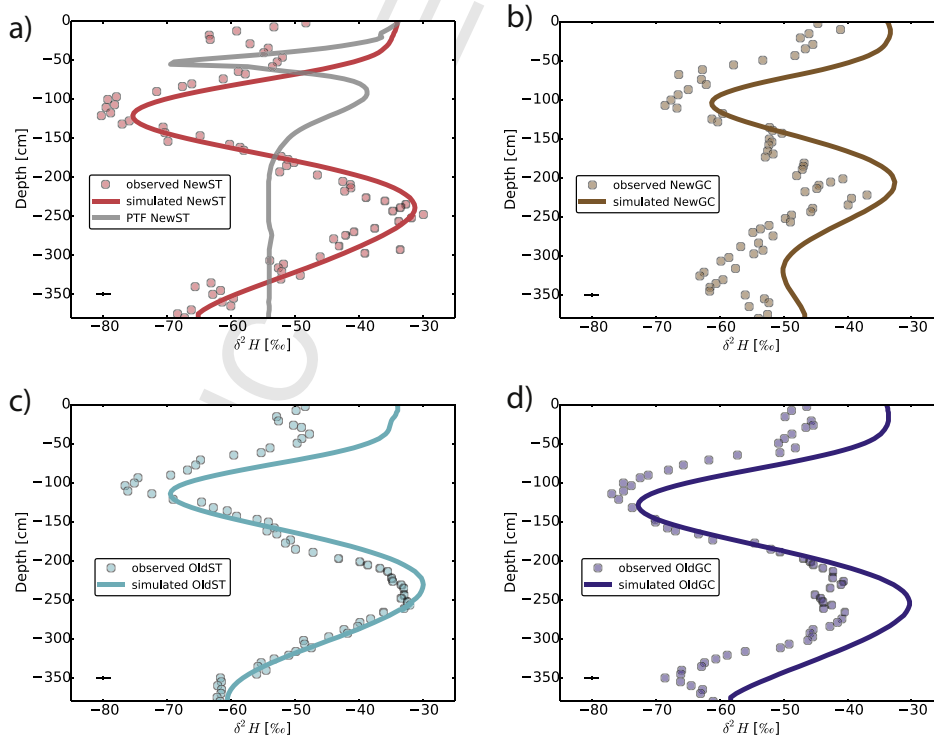


**Fig. 4.** Observed (points) and simulated (lines) deuterium composition in the pore waters of the four different study sites. For the site NewST (a), also the simulation using a pedotransfer function is shown (grey line). The accuracy of the  $\delta^2\text{H}$  analyses as the average standard deviation is shown with error bars below the legend.

**Table 2**

Soil hydraulic parameters derived by inverse modeling and the goodness of fit, given as the Kling–Gupta–efficiency (KGE).

Study site	$\theta_r$ ( $\text{cm}^3 \text{cm}^{-3}$ )	$\theta_s$ ( $\text{cm}^3 \text{cm}^{-3}$ )	$\alpha$ ( $\text{cm}^{-1}$ )	$n$ (–)	$K_s$ ( $\text{cm d}^{-1}$ )	$\lambda$ (cm)	KGE (–)
NewGC	0.116	0.343	0.0025	1.793	134.5	5.33	0.83
NewST	0.138	0.393	0.0010	2.307	327.5	3.28	0.86
OldGC	0.141	0.354	0.0013	2.068	393.3	4.61	0.87
OldST	0.106	0.545	0.0011	2.369	395.3	3.48	0.89

the other isotope profiles. NewST had a peak of depleted values in the top 30 cm, which was not present for the other isotope profiles. Beside these anomalies, in most of the depths, the  $\delta^{2}\text{H}$  values of the different sites did not differ more than the precision of the analysis of the pore water  $\delta^{2}\text{H}$  analysis ( $\delta^{2}\text{H} = 1.13\text{‰}$ ).

### 3.3. Calibration of the model

The inverse modeling procedure found soil hydraulic parameters that can reproduce the observed pore water  $\delta^{2}\text{H}$  data (Fig. 4). The KGE ranged between 0.83 and 0.89 and indicated a good fit between simulations and observations (Table 2). The first peak of depleted  $\delta^{2}\text{H}$  was in the simulated isotope profiles in the correct depth, but the isotopic composition was slightly enriched (max. +8‰) compared to the observations. The depth of the second peak was also well represented in the simulations and the deviation between observation and simulation exceeded only for OldGC the accuracy limit of the pore water  $\delta^{2}\text{H}$  analyses (Fig. 4d). Toward the profile bottom, the pore water  $\delta^{2}\text{H}$  data were well reflected for the sites NewST and OldST, while for the other two sites, the simulations were enriched compared to the observations. The simulations for NewGC tended generally to be enriched and the dampening of the signal was overestimated (Fig. 4c). The simulation for OldGC showed at the bottom of the soil profile an

offset toward increased percolation rates compared to the observations (Fig. 4d). An application of soil hydraulic parameters derived from the pedotransfer function by Schaap et al. (2001) for a silty soil showed that these parameters underestimate the percolation into the subsoil. In the simulation with pedotransfer functions, the precipitation input has even not reached the 200 cm depth plane after 5 years (grey line in Fig. 4a), while the inversely estimated parameters indicate faster percolation rates.

### 3.4. Water tracking

The simulations with the site specific calibrated soil hydraulic parameters showed that the water flow and solute transport does not differ a lot between the study sites (Fig. 5). The evapotranspiration was between 430 and 580  $\text{mm year}^{-1}$  over the simulation period and varied at most by 110  $\text{mm year}^{-1}$  between the sites in 2011 (Fig. 5a). The maximum differences between the sites for the recharge were given in 2012 with 140  $\text{mm year}^{-1}$ . Generally the recharge amount varied considerably between 55 and 290  $\text{mm year}^{-1}$  within the simulation period (Fig. 5b). The temporal dynamic of the mTT to pass the 100 cm depth plane was mainly driven by the precipitation pattern and ranged between 45 and 450 days (Fig. 5c). The ratio between the amount of the precipitation that ended up in recharge to the amount of evaporated water was governed by the seasonal

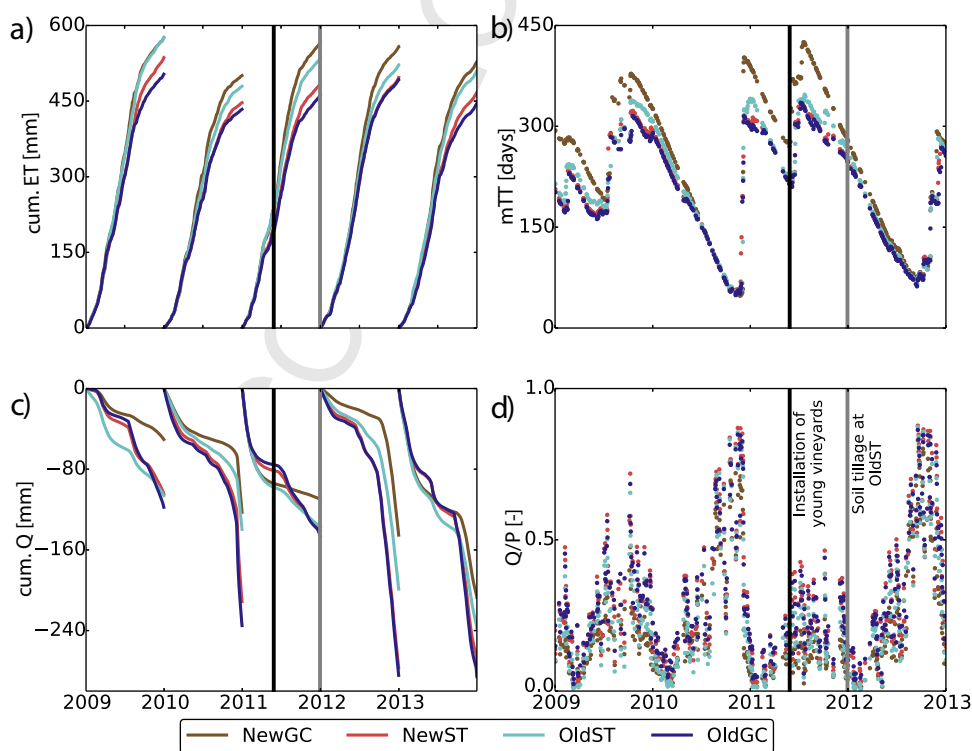


**Fig. 5.** Annual cumulative fluxes of evapotranspiration (a) and recharge (c), median travel time through the upper 100 cm (b), and the ratio between recharge and evapotranspiration (d). The vertical lines show the timing of the set-up of the young vineyards (dark grey, 24th of May 2011) and the timing of the soil tillage at one of the old vineyards (light grey, 30th of December 2011). The last year of the simulation (2013) is not shown for the travel time simulations (b and d), because the virtual tracer did not fully pass the 100 cm depth plane, which makes a calculation of the mTT and  $Q/P$  impossible.

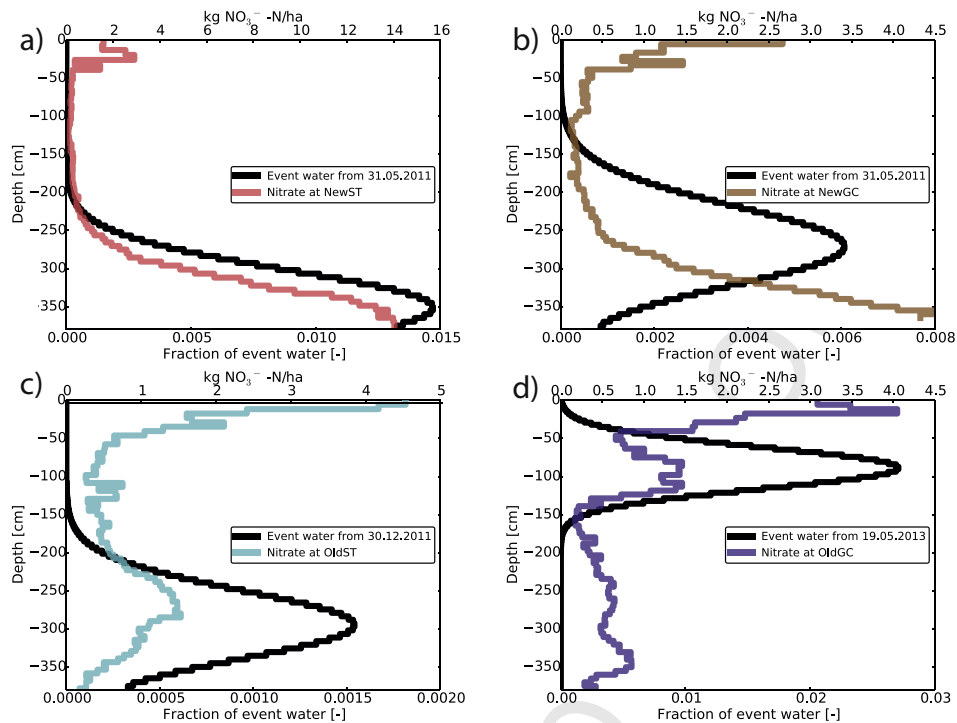


**Fig. 6.** Comparison between observed nitrate concentrations and simulated travel time distributions of water across the profile on the 4th of November 2013. The rainfall that was traced for the two young vineyards was from the 31st of May 2011, just after their set-up (a and b). For OldST, a rainfall from 30th of December 2011 was traced, which was just after soil tillage at that site (c). For OldGC, a rain event from the 19th of May 2013 was traced (d).

pattern of evapotranspiration (Fig. 5d). Up to 87% of the rain water that fell at the end of 2010 or 2012 became recharge, while water that entered the soil at the beginning of the years was more likely to leave the soil via evapotranspiration ( $Q/P < 0.1$ ). The rain water that fell in January needed relatively long to percolate through the upper 100 cm soil (mTT is between 250 and 400 days) and in the meantime, water could get transpired since it was still in the root zone.

In order to estimate the age of the pore water in the depths where elevated nitrate concentrations were found at the beginning of November 2013, we computed the distribution of water of several rainfall events (Fig. 6). For NewST, the precipitation input after the set-up of the vineyard (31st of May 2011) was traced. The simulation showed that the rainfall from the end of May 2011 reached after 2.5 years soil depths between 250 cm and >380 cm (Fig. 6a). The peaks of the traced precipitation water and the nitrate concentrations coincided at about 350 to 380 cm depth. For NewGC, where the fit between observed and simulated pore water  $\delta^{2}\text{H}$  was not as good as for the other three sites, also the fit between observed elevated nitrate concentration and the distribution of the precipitation input after the set-up of the vineyard did not match very well (Fig. 6b). The peak in the distribution of the rainwater from the 31st of May 2011 was located above the peak of the nitrate concentration. Thus, the simulated percolation process seemed to be slower than the observed nitrate displacement.

At OldST, elevated nitrate concentrations was between 220 and 350 cm. Tracing of the water of a precipitation event just after soil tillage at the end of 2011 showed that the rainfall of that time has reached exactly the depths of elevated nitrate concentrations (Fig. 6c). At OldGC, no tillage took place, but still, an elevated nitrate concentration was found between 80 and 130 cm depth. The pore water in these depths was mainly rainwater from May 2013 according to our simulations (Fig. 6d). However, no tillage was reported for May 2013 and thus, the origin of the nitrate cannot be referred to a certain management practice.

## 4. Discussion

### 4.1. Water stable isotopes

The observed pore water  $\delta^{2}\text{H}$  profiles show how the isotopic signal of the rain water over time is preserved in the unsaturated soil profile. However, the input signal is dampened due to mixing processes. For example, the depleted  $\delta^{2}\text{H}$  values from the winter 2012/2013 that reached values as deep as  $-100$  to  $-120\text{‰}$  are not present in the isotope profiles. Therefore, the percolation does not follow piston flow processes, but mixing of newly introduced water with “old” water takes place. The isotope profiles seem to directly reflect the seasonal variation of the isotopes in the rainfall. However, due to the dry and warm winter 2011/2012, it is not possible to simply refer the peak of isotopic enriched water to a

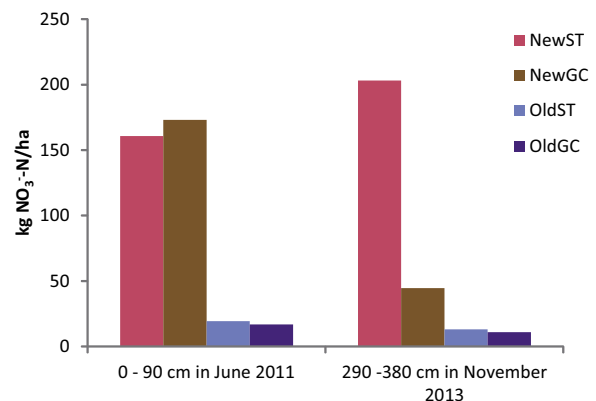


**Fig. 7.** Nitrate in the topsoil in June 2011 and in the subsoil in November 2013 at the newly established vineyards with soil tillage (red) and green cover (brown) and the vineyards in yield with soil tillage (light blue) and green cover (dark blue). (For interpretation of the references to color in this figure legend, the reader is referred to the web version of this article.)

summer and the depleted peak of isotopic depleted water below to the subsequent winter. During the winter of 2011/2012, little precipitation occurred and the rainwater was relatively enriched compared to the other winters in the simulation period (Fig. 1). Consequently, a peak of depleted water did not establish in the isotope profiles. Instead, pronounced rainfall in spring and summer introduced water with an enriched isotopic signal into the profile. As a result, the peaks of isotopic enriched pore waters in about 250 cm depth are wider, since they do not consist of water that fell within one summer, but water between the summer 2011 and the summer 2012.

The isotope profiles of 380 cm depth hold high information contents, because they are shaped by the hydrological processes of the last 3 years. Thus, the applied inverse modeling approach, which made use of the isotope profile data, has a solid base. The fact that the deviation between observed and simulated data is relatively small indicates that the major processes were reflected in the soil physical modeling. Nevertheless, the results for the site NewGC show the limits of the approach, since the simulated pore water  $\delta^2\text{H}$  data is shifted toward more isotopic enriched water compared to the observations. The isotope profile at NewGC differs from the other sites by less pronounced isotopic peaks and also the soil hydraulic parameters derived by inverse modeling differ from the other sites. However, it seems that the parameter set for NewGC does not reflect adequately the water flow and transport processes, but underestimates the percolation rates. The deviation between observed and simulated pore water  $\delta^2\text{H}$  data in the upper 50 cm at all sites is due to missing isotopic input data for the last four month of the simulation period. The assumed constant concentration does not reflect the isotopic composition of the rainfall. However, compared to the long simulation period of over five years, the information of the upper 50 cm does not play a big role for the inverse modeling approach.

The water balance simulations show that the model parameters result generally in a realistic representation of the vadose zone processes. The annual evapotranspiration of around 500 mm are close to evapotranspiration estimates with the aerodynamic profile method based on measured turbulent heat fluxes in a nearby scots pine forest (Imbery, 2005). Regarding the recharge fluxes, average values of 300 mm per year are reported for the study region (LUBW, 2008), which is in line for our simulated recharge fluxes for wet years (2012 and 2013). However, in relatively dry years like 2009 and 2011, the recharge flux is likely to be lower according to our simulations. The application of pedotransfer functions does not capture the hydrological processes, since it failed to simulate the observed pore water  $\delta^2\text{H}$  data. Also the common approach to infer travel times through the vadose zone by lumped transport models (e.g., Maloszewski et al., 2006), would not have been applicable, since these models require time series of flow concentrations of tracer data. Such data are difficult to collect in the field at depths deeper than 300 cm.

#### 4.2. Nitrate-N below vineyards

The nitrate sampling showed clearly that there are elevated nitrate concentrations under young vineyards compared to old vineyards. The elevated nitrate concentrations at NewST can be referred to water input into the soil profile that happened just after the set-up of the vineyards. For NewGC, the simulation result cannot directly relate the high nitrate concentration to the time of the set-up of the vineyards. The mismatch for NewGC is due to a representation of the soil hydraulic parameters that cannot reflect properly the water flow and solute transport processes. For OldST, the fit between elevated nitrate concentrations and the distribution of the rainwater that fell just after soil tillage in winter shows the impact of soil tillage for nitrate leaching. Even though the

nitrate loads are relatively low, they clearly show higher values compared to OldGC, where no tillage was applied. In contrast, OldGC shows elevated nitrate concentrations at about 100 cm depth, which cannot be referred to soil tillage, but stems from nitrate mineralization in May 2013 according to our simulations.

The applied method, where the rainwater was traced through the soil profile, cannot tell us directly about the fate of nitrate under vineyards. We follow the water flow with an ideal tracer. Thus, we do not consider any turnover processes that might happen with nitrate and uptake by the vegetation follows one-to-one with the water uptake. Nevertheless, the simulations of tracing rainwater show at what time the soil water of elevated nitrate concentrations in the subsoil was mineralized in the topsoil. The successful relation between age dating of the pore water and the mineralization of nitrate in the topsoil shows the potential of pore water stable isotope data for investigating vadose zone travel times.

We can infer that nitrate does not only get mineralized in the topsoil, but also leaches downwards over the years, because the elevated nitrate-N concentration in the subsoil coincides with the water distribution of the rain after the set-up of the vineyard for NewST. Although nitrate was already mineralized at the sites NewST and NewGC due to plowing about 6 months before the set-up of the young vineyard, the differences in management practice between the two study sites started with the sowing a green cover in every second interrow at NewGC after the set-up of the young vineyards. Therefore, we chose to trace the rainwater of that moment. Since nitrate has passed the rooting zone, the observed nitrate will reach the groundwater. A comparison between the nitrate concentrations in the upper 90 cm after the set-up of the young vineyards (Erhardt and Riedel, 2013) in June 2011 with the nitrate concentrations in the lowest 90 cm of the profile (290–380 cm) in November 2013 shows that the same amount of nitrate was leached down into the subsoil under NewST (Fig. 7). Thus, the nitrate concentration in the subsoil exceeds by far the control value of  $90 \text{ kg NO}_3^- \text{-N ha}^{-1}$  for the upper 90 cm soil depth as defined by the Umweltministerium (2001). In contrast, under NewGC, much of the nitrate that was mineralized in the top soil before and during the set-up of the vineyards was taken up by the seeded green cover before it could leach toward the subsoil. In addition, in contrast to NewST, no further nitrate mineralization due to tillage took place at NewGC. Consequently, in the profile of NewGC, there are no nitrate concentrations that reach the threshold. Also the soils under old vineyards are always below the control value of  $90 \text{ kg NO}_3^- \text{-N ha}^{-1}$  for 90 cm soil depth.

#### 5. Conclusion

The sampling of nitrate in soil down to 380 cm below old and young vineyards showed that the differences of soil tillage practice to permanent green cover are not limited to the usually sampled upper 90 cm. The pore water  $\delta^2\text{H}$  data could be reproduced with the soil physical model for three out of the four considered sites. The application of the model for the three sites to date the origin of the nitrate supported the hypothesis regarding the implication of management practices in viticulture. The nitrate that is mineralized due to soil tillage in the topsoil leaches into the subsoil where it eventually enters the groundwater. This is true for old vineyards, where elevated nitrate concentrations can be related to tillage during the winter, the dormant season, when the vegetation does not use nitrate. However, the nitrate loads are generally relatively low under old vineyards and the groundwater contamination seems to be little from these sites. Though, below young vineyards, where the interrows between the grapevines were kept free of vegetation after the set-up of the vineyards, the nitrate concentration in the subsoil indicates a pollution of the groundwater.

However, newly established vineyards amounted to only 2.4% of the area under vines in Baden in 2012 (Bärmann et al., 2013). Nevertheless, this impact can be significantly lowered due to sowing of a green cover after the set-up of the vineyards. This way, much of the mineralized nitrate is taken up before it can leach into the subsoil. Thus, we confirm with our study the current recommendations of sowing a green cover, at least every second interrow after planting, between young grapevines. Since green cover can also have devigorating effects on vines (Guerra and Steenwerth, 2012) and young vines do not widely spread root system like in old vineyards, winegrowers must respond to dry conditions during the growing season. However, in winter, the soil of new established vineyards must be covered with vegetation. Not only to reduce the impact on groundwater, but also to prevent soil erosion. Furthermore, the periodical soil tillage can have an impact on nitrate leaching and should therefore be applied in periods, where travel times in the root zones are likely to be long and vegetation is active. That way, nitrate that is mineralized is likely to travel long time within the rooting zone and can potentially be used by the vegetation before it leaches toward the groundwater.

## Acknowledgements

We thank Franziska Zieger and Begona Lorente Sistiaga for the support in the field during soil sampling and pore water stable isotope analysis in the laboratory, Barbara Herbsritt for the support in the laboratory at the Chair of Hydrology, and Jutta Fröhlin for the nitrate analysis at the State Institute for Viticulture and Enology Freiburg. We thank two anonymous referees for reviewing our manuscript.

## References

- Bärmann, E., Wolf, S., Krebs, H., 2013. Strukturdaten zum Jahrgang 2012: weißwein legt um rund 70 ha zu. *Badische Winzer* 8, 26–31.
- Duan, Q., Sorooshian, S., Gupta, V.K., 1994. Optimal use of the SCE-UA global optimization method for calibrating watershed models. *J. Hydrol.* 158 (3), 265–284.
- Erhardt, M., Riedel, M., 2011. Weiterentwicklung einer standort- und witterungsabhängigen Bodenpflege und stickstoffdüngung im Weinbau: beratungs- und forschungsprojekt in Südbaden. *Landinfo* 3, 17–18.
- Erhardt, M., Riedel, M., 2012. Wasserrahmenrichtlinie: maßnahmen im Weinbau. *Deutsche Weinbau* 9, 20–22.
- Erhardt, M., Riedel, M., 2013. Junganlage: bodenpflege & stickstoffmanagement. *Deutsche Weinbau* 13, 24–27.
- Erhardt, M., Fröhlin, J., Schies, W., Riedel, M., 2012. Bodenpflege und stickstoffdüngung. *Badische Winzer* 25–28.
- Erhardt, M., Müller, T., Riedel, M., 2013. Green cover in new established vineyards: benefits for water protection, in: GiESCO (Ed.), Proceedings of the 18th International GiESCO Symposium. *Ciencia e Tecnica Vitivinicola* 2, 1052–1055 pp.
- European Council, 1991. Directive 91/676/EEC of 12 December 1991 Concerning the Protection of Waters Against Pollution Caused by Nitrates from Agricultural Sources 34. European Council.
- European Council, 2000. Directive 2000/60/EC of the European Parliament and of the Council Establishing a Framework for the Community Action in the Field of Water Policy 43. European Council.
- European Council, 2006. Directive 2006/118/EC of the European Parliament and of the Council of 12 December 2006 on the Protection of Groundwater Against Pollution and Deterioration 49. European Council.

- Feddes, R.A., Kowalik, P.J., Zaradny, H., 1978. Simulation of Field Water Use and Crop Yield. Simulation Monographs. Centre for Agricultural Publishing and Documentation, Wageningen.
- Guerra, B., Steenwerth, K., 2012. Influence of floor management technique on grapevine growth, disease pressure, and juice and wine composition: a review. *Am. J. Enol. Viticult.* 63 (2), 149–164. doi:<http://dx.doi.org/10.5344/ajev.2011.10001>.
- Hoffman, G., van Genuchten, M., 1983. Soil properties and efficient water use: water management for salinity control. In: Taylor, H., Jordan, W., Sinclair, T. (Eds.), Limitations and Efficient Water Use in Crop Production. American Society of Agronomy, Madison, WI, pp. 73–85.
- Imbery, F., 2005. Langjährige Variabilität der aerodynamischen Oberflächenrauigkeit und Energieflüsse eines Kiefernwaldes in der südlichen Oberrheinebene (Hartheim). Dissertation, Freiburg i. Br.
- Kling, H., Fuchs, M., Paulin, M., 2012. Runoff conditions in the upper Danube basin under an ensemble of climate change scenarios. *J. Hydrol.* 424–425, 264–277. doi:<http://dx.doi.org/10.1016/j.jhydrol.2012.01.011>.
- LTZ, 2001. Untersuchung von Bodenproben auf den Nitratgehalt. Landwirtschaftliches Technologiezentrum Augustenberg.
- LTZ, 2013. SchALVO-Nitratbericht: Ergebnisse der Beprobung 2013. Ministerium für Ländlichen Raum und Verbraucherschutz Baden-Württemberg, Stuttgart, Germany.
- LUBW, 2008. Gefährdeter Grundwasserkörper 16.6 Kaiserstuhl–Breisgau: Bewertung und Erfordernis weitergehender Maßnahmen. Landesanstalt für Umwelt, Messungen und Naturschutz Baden-Württemberg, Karlsruhe, Germany.
- LUBW, 2009. Gefährdete Grundwasserkörper in Baden-Württemberg Zusammenfassung und Erfordernis weitergehender Maßnahmen: Rechtlicher Rahmen, Methodik und Ergebnisse—wasserfachliche Bearbeitung. Landesanstalt für Umwelt, Messungen und Naturschutz Baden-Württemberg, Karlsruhe, Germany.
- Ritchie, J.T., 1972. Model for predicting evaporation from a row crop with incomplete cover. *Water Resour. Res.* 8 (5), 1204–1213. doi:<http://dx.doi.org/10.1029/WR008i005p01204>.
- Rupp, D., 1988. Rigolen von rebböden und die nitratauswaschung. *Deutsche Weinbau* 25–26, 1135–1137.
- Schaap, M.G., Leij, F.J., van Genuchten, M.T., 2001. ROSETTA: a computer program for estimating soil hydraulic parameters with hierarchical pedotransfer functions. *J. Hydrol.* 251 (3–4), 163–176. doi:[http://dx.doi.org/10.1016/S0022-1694\(01\)00466-8](http://dx.doi.org/10.1016/S0022-1694(01)00466-8).
- Šimunek, J., Sejna, M., Saito, H., Sakai, M., van Genuchten, M. Th., 2012. The HYDRUS-1D software package for simulating the one-dimensional movement of water, heat, and multiple solutes in variably-saturated media, Version 4.15, Riverside, California.
- Sprenger, M., Volkmann, T.H.M., Blume, T., Weiler, M., 2015. Estimating flow and transport parameters in the unsaturated zone with pore water stable isotopes. *Hydrol. Earth Syst. Sci.* 19 (6), 2617–2635. doi:<http://dx.doi.org/10.5194/hess-19-2617-2015>.
- Sprenger, M., Seeger, S., Blume, T., Weiler, M., 2016. Travel times in the vadose zone: variability in space and time. *Water Resour. Res.* (in revision).
- Stumpp, C., Stichler, W., Kandolf, M., Šimunek, J., 2012. Effects of land cover and fertilization method on water flow and solute transport in five lysimeters: a long-term study using stable water isotopes. *Vadose Zone J.* 11 (1) doi:<http://dx.doi.org/10.2136/vzj2011.0075>.
- Umweltministerium, 2001. Verordnung des Umweltministeriums über Schutzbestimmungen und die Gewährung von Ausgleichsleistungen in Wasser- und Quellenschutzgebieten (Schutzgebiets- und Ausgleichs-Verordnung—SchALVO) Vom 20. Februar 2001: SchALVO.
- van Genuchten, M.T., 1980. A closed-form equation for predicting the hydraulic conductivity of unsaturated soils. *Soil Sci. Soc. Am. J.* 44 (5), 892–898.
- Wassenaar, L., Hendry, M., Chostner, V., Lis, G., 2008. High resolution pore water  $\delta^{2}\text{H}$  and  $\delta^{18}\text{O}$  measurements by  $\text{H}_2\text{O}$  (liquid)– $\text{H}_2\text{O}$  (vapor) equilibration laser spectroscopy. *Environ. Sci. Technol.* 42 (24), 9262–9267. doi:<http://dx.doi.org/10.1021/es082065s>.
- Wesseling, J.G., 1991. Meerjarige simulaties van grondwateronttrekking voor verschillende bodmprofielen, grondwatertrappen en gewassen met het model SWATRE. Report 152, Wageningen, Netherlands.

533  
534  
535  
536  
537  
538  
539  
540  
541  
542  
543  
544  
545  
546  
547  
548  
549  
550  
551  
552  
553  
554  
555  
556  
557  
558  
559  
560  
561  
562  
563  
564  
565  
566  
567  
568  
569  
570  
571  
572  
Q9 573  
574  
575  
576  
577  
578  
Q10 579  
580  
581  
582  
583  
584  
585  
586  
587  
588  
589  
590  
591  
592  
593  
Q11 594  
595